


Article

Simple and Equipment-Free Paper-Based Device for Determination of Mercury in Contaminated Soil

Hikmanita Lisan Nashukha^{1,2}, Jirayu Sitanurak^{1,2}, Hermin Sulistyarti³, Duangjai Nacapricha^{1,2} and Kanchana Uraisin^{1,2,*} 

¹ Flow Innovation-Research for Science and Technology Laboratories (Firstlabs), Mahidol University, Rama 6 Road, Bangkok 10400, Thailand; hikmanitalisan@gmail.com (H.L.N.); jsitanurak@gmail.com (J.S.); dnacapracha@gmail.com (D.N.)

² Department of Chemistry and Center of Excellence for Innovation in Chemistry, Faculty of Science, Mahidol University, Rama 6 Road, Bangkok 10400, Thailand

³ Department of Chemistry, Faculty of Science, Brawijaya University, Jl. Veteran Malang 65145, Indonesia; sulistyarti@yahoo.com

* Correspondence: kanchana.ura@mahidol.ac.th; Tel.: +66-2-201-5125

Abstract: This work presents a simple and innovative protocol employing a microfluidic paper-based analytical device (μ PAD) for equipment-free determination of mercury. In this method, mercury (II) forms an ionic-association complex of tetraiodomercurate (II) ion (HgI_4^{2-}) using a known excess amount of iodide. The residual iodide flows by capillary action into a second region of the paper where it is converted to iodine by pre-deposited iodate to liberate $\text{I}_{2(g)}$ under acidic condition. Iodine vapor diffuses across the spacer region of the μ PAD to form a purple colored of tri-iodide starch complex in a detection zone located in a separate layer of the μ PAD. The digital image of the complex is analyzed using ImageJ software. The method has a linear calibration range of 50–350 mg L^{-1} Hg with the detection limit of 20 mg L^{-1} . The method was successfully applied to the determination of mercury in contaminated soil and water samples which the results agreed well with the ICP-MS method. Three soil samples were highly contaminated with mercury above the acceptable WHO limits (0.05 mg kg^{-1}). To the best of our knowledge, this is the first colorimetric μ PAD method that is applicable for soil samples including mercury contaminated soils from gold mining areas.

Keywords: tetraiodomercurate; mercury; paper-based; iodometry; soil; water



Citation: Nashukha, H.L.; Sitanurak, J.; Sulistyarti, H.; Nacapricha, D.; Uraisin, K. Simple and Equipment-Free Paper-Based Device for Determination of Mercury in Contaminated Soil. *Molecules* **2021**, *26*, 2004. <https://doi.org/10.3390/molecules26072004>

Academic Editor: Pawel Koscielniak

Received: 8 March 2021

Accepted: 29 March 2021

Published: 1 April 2021

Publisher's Note: MDPI stays neutral with regard to jurisdictional claims in published maps and institutional affiliations.



Copyright: © 2021 by the authors. Licensee MDPI, Basel, Switzerland. This article is an open access article distributed under the terms and conditions of the Creative Commons Attribution (CC BY) license (<https://creativecommons.org/licenses/by/4.0/>).

1. Introduction

Mercury is well known as one of the most toxic elements for organisms and human health. It is known that natural disasters such as volcano eruptions and forest fires can cause the release of mercury and contamination of the environment [1]. Nonetheless, emission of mercury from artisanal small-scale gold mining (ASGM) is the largest source of mercury emission in some developing countries [2,3], where mercury is used for amalgamation and purification of gold [4]. The US EPA methods for determination of mercury in water [5] and soil [6] are based on cold vapor atomic absorption spectrometry (cold vapor-AAS). For complicated matrices such as soil and sediment, a method employing use of an alkaline reagent (pH \approx 14), named Universol[®] was recently presented in association with cold vapor-AAS [7]. There are also other equipment-based methods that have been employed for these samples, such as high-performance liquid chromatographic method using chemiluminescence detection [8] and inductively coupled plasma mass spectrometric method or ICP-MS [9] for soil samples, as well as a resonance scattering spectroscopic method [10] for water samples.

Among equipment-based techniques, colorimetric spectrometry is still the favored technique for the determination of mercury because of its simplicity and availability of cost-effective instruments. The water soluble Michler's thioketone reagent (4,4'-Bis-(dimethylamino)-

thiobenzophenone) has been used for detection of mercury but the method could be interfered by other metal ions, such as Cr(III), Fe(III) and Cu(II) [11]. Several selective reagents have also been proposed for the determination of mercury. However, most chromogenic reagents are insoluble in water, e.g., 1-[(5-Benzyl-1,3-thiazol-2-yl)diazenyl]naphthalene-2-ol [12], dithizone [13], 2-(3-hydroxy-1-methylbut-2-enylideneamino) pyridine-3-ol [14] and 2,4-bis (4-phenylazophenylaminodiazo) benzenesulfonic acid [15]. In order to improve the solubility of these organic reagents, the reaction has to be carried out in a micellar system of sodium dodecyl sulphate [13] or Triton X-100 [15]. Functionalized gold nanoparticles (AuNPs) with dithioerythritol [16], 3, 5-dimethyl-1-thiocarboxamidepyrazole (Pzl) [17] or mercaptophenyl boronic acid (MPBA) [18] have also been presented for colorimetric/spectrometric detection of mercury. Nonetheless, for low- and middle-income countries (in Asia, Africa, the Pacific and South America) where emissions of mercury are mainly from gold mining activities, equipment-free and low-cost devices for mercury determination are needed as tools for monitoring the anthropogenic emission at point source and the extent of the spread of the contamination.

Microfluidic paper-based analytical devices (μ PADs) [19–23], as well as reagent impregnated-paper strips/devices, are analytical tools that is in line with the strategy of equipment-free analysis using low-cost devices. For producing μ PADs, patterns are drawn on the paper substrate using various hydrophobic materials to act as barriers to control the fluid flow on the paper. For mercury, there are some interesting paper-based devices that have been presented for colorimetric detection of mercury (as Hg^{2+}) with photographic image analysis [24–28]. Patidar et al. presented two synthesized rhodamine derivatives for colorimetric detection of Hg^{2+} (and Cr^{3+}) on paper strips and cellulose acetate membrane [24]. A resorufin thionocarbonate signaling probe for Hg^{2+} was recently synthesized by the group of Chang [25]. Hg^{2+} induces cleavage reaction of thionocarbonate moiety of the probe leading to a prominent color change from yellow to pink. This probe was later incorporated into a wax printed μ PAD for selective detection of Hg^{2+} . Nanoparticles have been utilized by various groups to develop sensitive colorimetric paper-based analytical devices (PADs)/ μ PADs for quantifying Hg^{2+} [26–30]. Han et al. presented a paper chip for Hg^{2+} detection based on the enzyme-like catalytic activity of gold nanoparticles (AuNPs) that is enhanced by the formation of Au-Hg amalgam for the reaction between 3,3',5,5'-tetramethylbenzidine (TMB) and H_2O_2 [29]. The color intensity of the chromogenic peroxidase substrate (TMB image) corresponds to the concentration of Hg^{2+} . Silver nanoparticles (AgNPs) were also employed as colorimetric sensors for PADs/ μ PADs [26,27,30]. Hg^{2+} is reduced by AgNPs which leads to disintegration of the AgNPs into smaller particles and formation of Hg^0 [26]. Subsequent deposition of Hg^0 onto AgNPs gives Ag-Hg amalgam particles resulting in the change in the color intensity which is dependent on the concentration to Hg^{2+} [30]. Pourresza et al. presented a colorimetric paper-based analytical device incorporating synthesized curcumin nanoparticles (CcNPs) for quantifying Hg^{2+} [28]. Complex formation between Hg^{2+} and CcNPs leads to the fading of the yellow color which is used for the determination of Hg^{2+} . A distance-based readout μ PAD for determination of Hg^{2+} was also presented by Cai et al. [31]. The reaction between Hg^{2+} and dithizone in NaOH solution forms an insoluble colored complex in the paper channel. The length of the pink reaction band increases linearly with the concentration of Hg^{2+} . Most of these PAD/ μ PAD methods were tested to analyze water samples spiked with mercury [25–31]. To the best of our knowledge, there has been no PAD/ μ PAD previously presented for detection of mercury in soil.

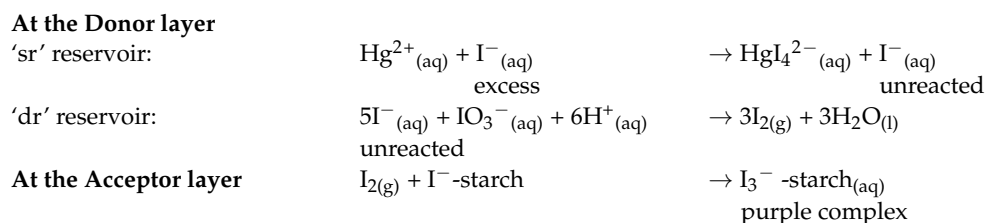
Therefore, this work presents a μ PAD as tool for analyzing soil heavily contaminated with mercury. The μ PAD can be used to identify the source and the dispersion of mercury emission from gold mining activities. The μ PAD method is also appropriate for assessing inactive gold mines for persistence of the release of mercury to villages surrounding the mines. The μ PAD was fabricated based on the concept of membraneless gas-separation microfluidic paper-based analytical device (membraneless gas separation μ PAD) that was introduced in 2016 by Phansi et al. [32]. This work quantitates mercury via formation of

tetraiodomercurate(II) ion (HgI_4^{2-}) with a known amount of excess iodide. This ionic-association complex is formed in the sample reservoir of the “donor layer”. The residual iodide reagent then flows via capillary action to react with iodate and acid to generate iodine (I_2) in the neighboring reservoir of the “donor layer”. I_2 vaporizes from this reservoir through the headspace (the spacer layer) to form a purple complex of tri-iodide starch in the detection reservoir of the third “acceptor layer”. Photographic images of the purple complex are analyzed using ImageJ to obtain the color intensities for the quantitation of mercury. Our device serves the needs of low- and middle-income countries with limited resources in the mining areas as simple and low-cost tool capable for mercury determination in samples with complicated matrix such as soil. The device is readily implemented to assess crisis and situation of mercury emission. Production cost of the mercury μPAD is very cost-effective (7 US\$/100 devices) [33]. The reagents are common and are supplied worldwide at reasonably low in costs (potassium iodide, potassium iodate, sulfuric acid and starch). In addition to the use of the mercury standards (which is unavoidable in any mercury determination), our method does not contribute hazardous waste to the environment.

2. Results and Discussion

2.1. Principle of Indirect Colorimetric Detection of Mercury

Mercuric ion reacts with iodide ion to form a stable complex of tetraiodomercurate (HgI_4^{2-} , $K_f = 7.4 \times 10^{12}$) [34]. The complex is a colorless compound which cannot be detected using a digital camera. In order to generate intense visible color, the iodometric reaction was employed. The detection principle is based on the following reactions:



The first step of the reaction occurs in the donor layer ‘D’ at the sample reservoir ‘sr’ (Figure 1b) where the stable complex of HgI_4^{2-} is formed. The remaining I^{-} flows to the donor reservoir ‘dr’ and is oxidized by acidic iodate to produce iodine gas ($\text{I}_{2(\text{g})}$). The gas diffuses across the spacer layer to react with the iodide-starch reagent producing the purple tri-iodide starch complex on the acceptor layer ‘A’. The higher the concentration of $\text{Hg}(\text{II})$, the less amount of iodide will remain in the donor reservoir ‘dr’, resulting in decrease of production of iodine gas and consequently decrease in the color intensity of the I_3^{-} -starch complex, as can be visually observed. The color of the complex at the acceptor zone (layer A in Figure 1) is recorded using the digital camera and the image analyzed using ImageJ software. The RGB (red, green, blue) intensity values were evaluated. It was found that the data for the green intensity scale provided the highest sensitivity of the linear calibration line (see Method S1, Figure S1 and the discussion in the Supplementary data for the selection of the green color intensity).

2.2. Optimization of Physical Parameters of the μPAD

Three physical parameters were optimized using standard $\text{Hg}(\text{II})$ solutions in the range of 50–350 mg L^{-1} by following the protocol illustrated in Figure 2. The sensitivity, i.e., the slope of the calibration line, was the target of the optimization process.

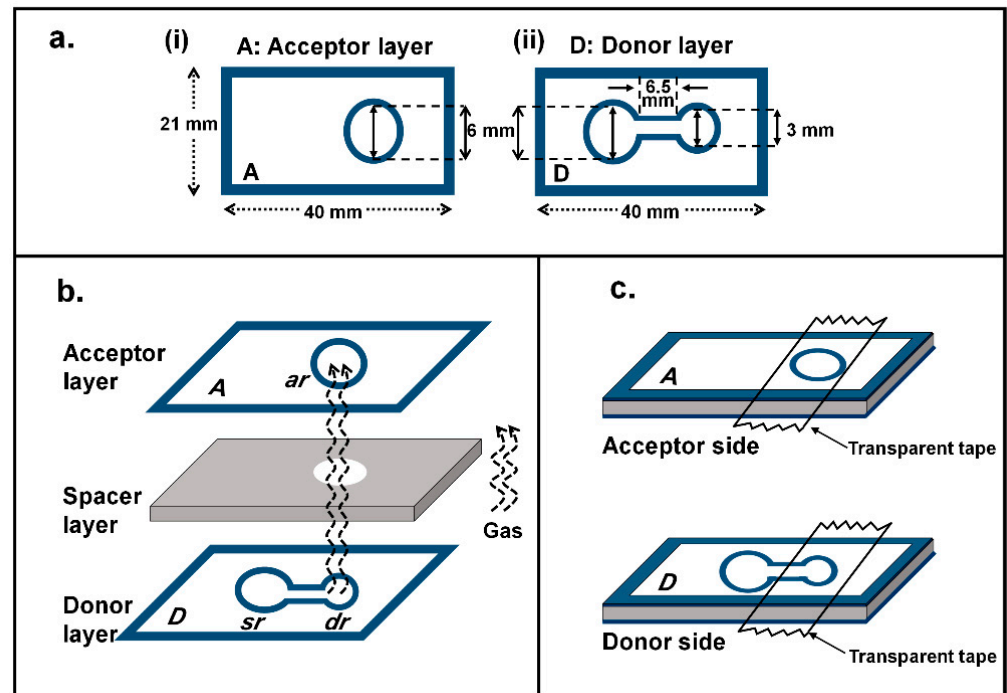


Figure 1. (a) The μ PAD pattern: (i) acceptor layer A with circular-shaped barrier and (ii) donor layer D with dumbbell-shaped barrier. (b) The three layers of the membraneless gas-separation μ PAD, showing alignment of the donor layer, the spacer layer with circular hole and the acceptor layer. (c) 3D-view of assembled device from both the acceptor and donor sides, with position of the transparent tapes.

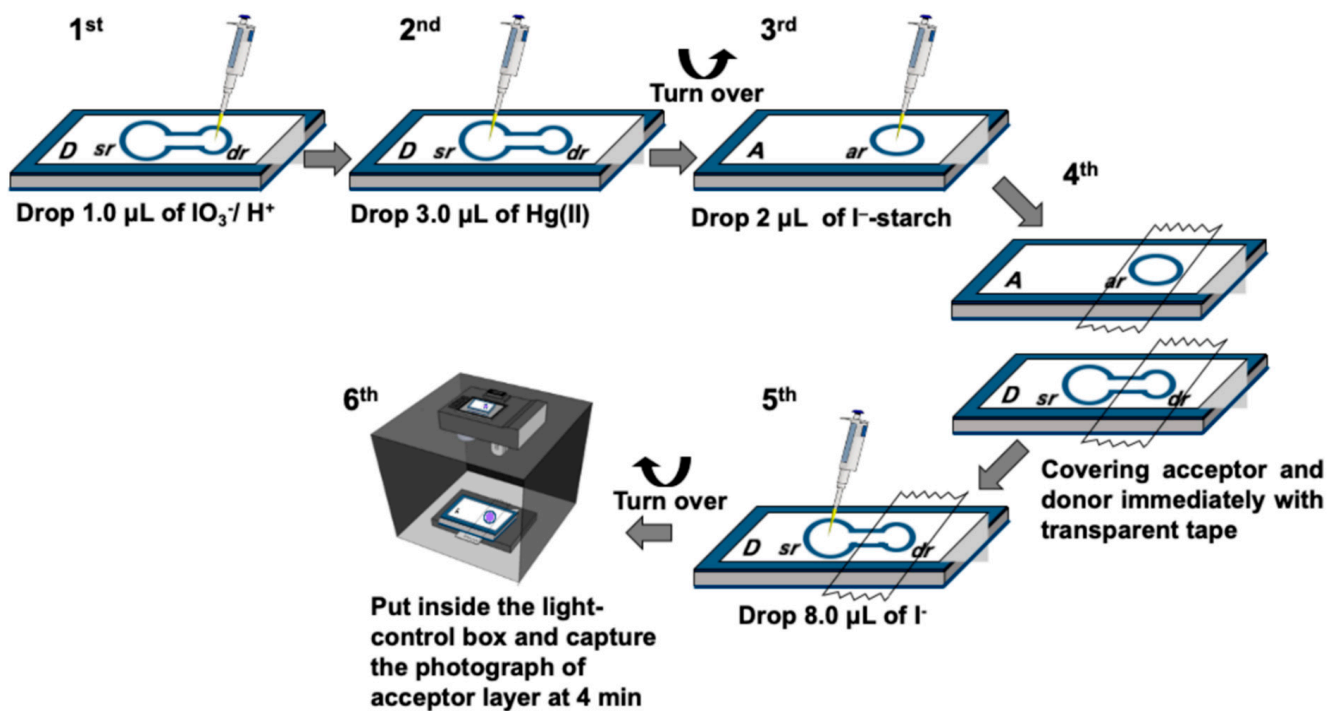
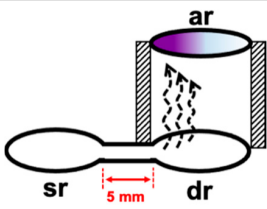

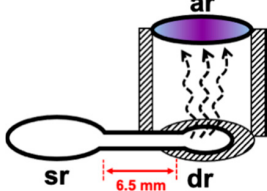
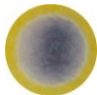


Figure 2. Illustration of the operating steps for the determination of mercury using the membraneless gas-separation μ PAD.

2.2.1. Diameter of Donor Reservoir

In the previous work of membraneless gas-separation μ PADs reported by Phansi et al. for determination of volatile (ethanol) and non-volatile compounds (S^{2-} and NH_4^+) [32] three μ PADs with donor reservoir diameters of 6, 8 and 10 mm were tested. They found that the volume of the air gap increases with an increase in the donor reservoir diameter which results in a decrease in the sensitivity of measurements. Therefore, the smallest diameter of the donor reservoir (6 mm) was selected and this diameter was also used as the size of the acceptor reservoir. When this dimension was used in this work, the color of the complex developed towards one side of the acceptor reservoir (see photographs in Table 1). As illustrated by the drawings in Table 1, for the donor reservoir with larger diameter (6 mm), it appears that iodine is generated mostly at the entrance of the donor reservoir 'dr'. This gives rise to uneven distribution of the color and low precision of the mean of the color intensity value of the designated area of the acceptor reservoir. To solve this problem, the diameter of the donor reservoir was reduced to 3 mm and the length of the connecting channel was slightly increased from 5 to 6.5 mm. In the fabrication of the membraneless gas-separation device, the center of the 3 mm donor reservoir 'dr' was aligned with the center of the acceptor reservoir, as shown in the drawing in Table 1. With use of the smaller diameter of 3 mm, homogeneity of color distribution, as well as higher sensitivity of analysis, was achieved. Therefore, the donor reservoir diameter of 3 mm was selected in further optimization study.

Table 1. Effect of size of diameter of donor reservoir on homogeneity of color distribution at the acceptor reservoir and on the sensitivity of analysis.

Diameter of Donor Reservoir	Working Range ($mg\ L^{-1}\ Hg$)	Linear Equation	Schematic Diagram of the Experimental Study	Image of the Acceptor Reservoir (6 mm) for $150\ mg\ L^{-1}\ Hg$
6 mm	50–350	Intensity = $(4.0 \pm 0.5) \times 10^{-2} C_{Hg(II)} + (123.7 \pm 1.1)$		
3 mm	50–350	Intensity = $(5.5 \pm 0.5) \times 10^{-2} C_{Hg(II)} + (127.9 \pm 1.1)$		

2.2.2. Effect of Reaction Time

In this work, the reaction time is defined as the time period from the addition of the iodide solution into the sample reservoir 'sr' (Step 5 in Figure 2) to the recording of the image of the detection area (Step 6). The reaction time was varied from 2 to 8 min, respectively. Figure 3a shows that the sensitivity significantly increased when the reaction time was increased from 2 min to 4 min. However, the sensitivity remained constant for reaction times of 6 and 8 min. This implied that the partial pressure of the iodine gas was attained within 4 min. Therefore, the minimum reaction time of 4 min was selected for further studies. However, in order to increase sample throughput, multiple analyses can be carried out since reaction time longer than 4 min does not affect the measurement.

2.2.3. Effect of Spacer Thickness

Effect of the spacer thickness of the μ PAD was also optimized. The spacer thickness was increased from 0.8 to 3.2 mm by increasing the number of layers of the 0.8 mm

mounting tape, respectively. The result in Figure 3b shows that the sensitivity significantly decreases with increasing spacer thickness. This may be due to the increased volume of the air-gap which will require more iodine to provide the same equilibrium partial pressure and, hence, less iodine reacting with the iodide-starch reagent. This effect was also observed in the previous report [35]. Thus, we selected 0.8 mm air gap in the further studies.

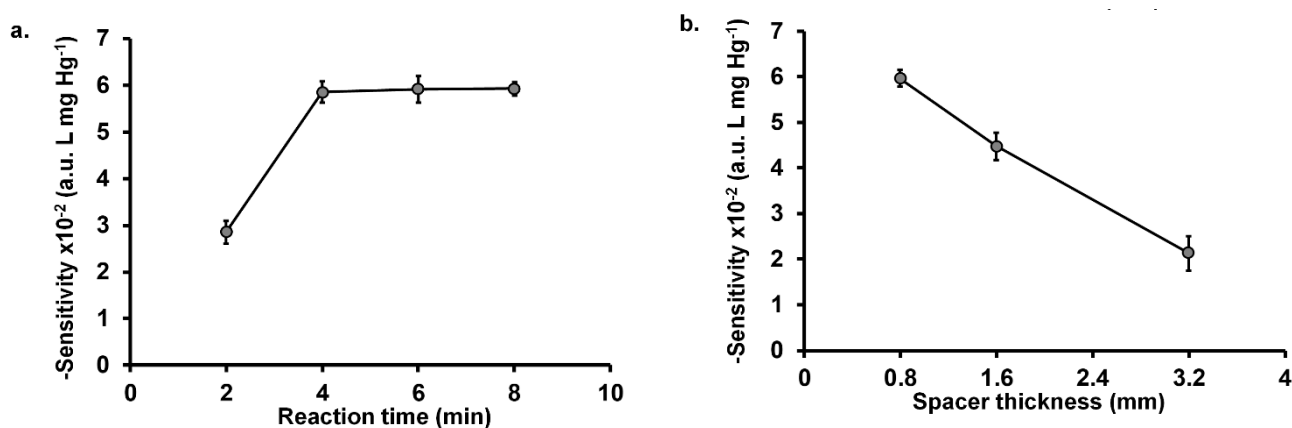


Figure 3. Effect of physical parameters on analysis of Hg(II): (a) reaction time and (b) spacer thickness. Experimental conditions: 0.2 mol L⁻¹ KIO₃ in 0.2 mol L⁻¹ H₂SO₄, 10 mmol L⁻¹ KI and 1% (w/v) of starch in 0.1 mmol L⁻¹ KI. For the spacer thickness study, the reaction time is 4 min.

2.3. Optimization of Chemical Parameters of μ PAD

2.3.1. Iodide Concentration

The determination of Hg(II) is based on the measurement of the iodide remaining after reaction with mercury in the sample. Therefore, the initial concentration of iodide is an important parameter as it will affect the amount of iodine gas produced and, thus, the formation of the I₃⁻-starch complex. The study was carried out using a standard solution of 150 mg L⁻¹ Hg(II) with the concentrations of potassium iodide varied from 5 to 14 mmol L⁻¹, respectively. As expected, increasing the initial concentration of iodide, the value of the green intensity of I₃⁻-starch complex also increased, corresponding with the amount of remaining iodide (Figure 4b). The images of the purple I₃⁻-starch complex are shown in Figure 4a. Measurements of the sensitivity of determination, using standard Hg(II) solutions from 50–350 mg L⁻¹, showed increasing sensitivity for iodide concentration up to 10 mmol L⁻¹. However, there is a steep decline at higher concentration of iodide (Figure 4b). Using large amount of initial iodide (>10 mmol L⁻¹), the green intensity did not significantly change with the concentrations of standard Hg(II) (50–350 mg L⁻¹). This showed that the amount of Hg(II) in the samples consumed only a small proportion of the initial iodide, resulting in calibration curves with low sensitivity. In fact, for loading of 8.0 μ L of 10 mmol L⁻¹ iodide (Step 5 in Figure 2) on to the previously applied Hg(II) standard (3.0 μ L, Step 2 in Figure 2) the amount of remaining iodide is 96% for 50 mg L⁻¹ Hg and 74% for 350 mg L⁻¹ Hg. Thus, 10 mmol L⁻¹ was selected because it provided the highest sensitivity.

2.3.2. The pH of Mercury Solution

The pH of the mercury solution was investigated to find the suitable value for the reaction of iodide to form the HgI₄²⁻ complex. Mercuric ion is unstable at high pH where the main species include HgOH⁺, Hg(OH)₂ and Hg(OH)₃⁻ [36,37]. Therefore, low pH was selected to have Hg²⁺ as the main species. Optimization was carried out using standard 150 mg L⁻¹ Hg in the pH range of 0.5 to 4. The results in Figure S2 (Supplementary data) shows that the green intensity value increased from pH 0.5 to pH 2 and then decreased. It was found that self-oxidation of iodide was taking place at extremely low pH producing iodine gas (at sample reservoir 'sr') at the same as reacting with mercury. Stable condition

was achieved at pH 1 and 2 (Figure S2). Kim et al. have reported that mercury in solution with +2 oxidation state has the highest stability at pH 2 and decreasing with increasing pH [37]. Thus, we selected pH 2 as the optimum pH for determination of mercury since it provides the highest green intensity with absence of self-oxidation of iodide.

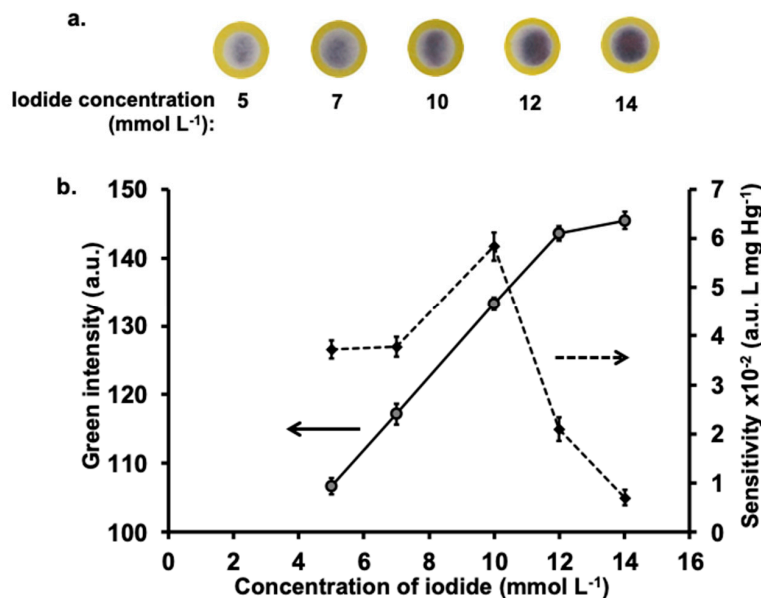


Figure 4. Effect of iodide concentration on analysis of Hg(II): (a) images of purple iodine-starch complex for various concentrations of iodide analysis using a standard solution of 150 mg L⁻¹ Hg and (b) plots of effect of iodide concentrations on the green intensity values (left ordinate) using a standard solution of 150 mg L⁻¹ Hg and sensitivity of Hg(II) analysis (right ordinate). Experimental conditions: 0.2 mol L⁻¹ KIO₃ in 0.2 mol L⁻¹ H₂SO₄, 10 mmol L⁻¹ KI, 1% (*w/v*) of starch in 0.1 mmol L⁻¹ KI and reaction time of 4 min.

2.4. Analytical Performance and Interference Study

2.4.1. Analytical Features

Using the optimal parameters (described above) and operating procedure (Section 3.4 and Figure 2), the linear working range was 50–350 mg L⁻¹ Hg, with coefficient of determination r^2 of 0.996 (Figure 5). The limit of detection (3σ of y-intercept/slope) and limit of quantification (5σ of y-intercept/slope; [38]) were 20 mg L⁻¹ and 33 mg L⁻¹ Hg, respectively. Thus, the method is applicable for determination of mercury in contaminated samples such as soil including water samples collected from gold mining areas. The contaminated water samples can be directly analyzed without any sample preparation step whereas the contaminated soil samples have to be digested prior to the analysis. The mercury contents in water and digested soil samples (concentration range of a hundred mg L⁻¹) are mutual with the calibration range. The repeatability of the proposed method was performed by measurement of standard Hg(II) solution of 150 mg L⁻¹ Hg for twelve replicates, with a %RSD of 2.2%. The determination of one mercury sample can be carried out within 10 min; however, the number of sample throughput can be increased with simultaneous analyses of samples.

2.4.2. Interference Study

The proposed μ PAD method was developed for the determination of mercury in soil and water samples from gold mining areas. Therefore, the effect of interfering species that are normally present in water and soil in such areas were investigated. According to the previous report of Malehase et al. in 2016 [39], several metal ions and anions have been found in soil and water samples in the gold mining area. These include iron (Fe), copper (Cu), chromium (Cr), cadmium (Cd), zinc (Zn), lead (Pb), silver (Ag), nitrate (NO₃⁻), sulfate

(SO_4^-) and chloride (Cl^-). Therefore, these and other ions (see Table 2) were investigated for their effect on the mercury analysis. A 50 mg L^{-1} of mercury standard solution was employed as the test solution which was spiked with various concentrations of each interfering species. In this work, the tolerance limit is defined as the highest concentration of the foreign species causing a change of the green intensity less than ± 1 SD (standard deviation) for the determination of 50 mg L^{-1} Hg standard solution. This SD value was 4.5% of the mean intensity. The results in Table 2 show that, among the metals ions, Fe(III) and Ag(I) show low levels of tolerance because Fe(III) acts as oxidizing agent of iodide ($E^0_{\text{Fe}^{3+}/\text{Fe}^{2+}} = 0.77 \text{ V}$, $E^0_{\text{I}_2/\text{I}^-} = 0.54 \text{ V}$) and Ag(I) can precipitate out with iodide ($\text{AgI}_{(s)}$; $K_{\text{sp}} = 8.3 \times 10^{-17}$). As for the anions, sulfide (S^{2-}) shows the lowest level of tolerance of 25 mg L^{-1} since sulfide has a high affinity for mercury to form $\text{HgS}_{(s)}$ ($K_{\text{sp}} = 2 \times 10^{-54}$) [34]. However, the tolerance concentrations of all substances are still higher than the reported levels in water and soil samples. Therefore, the proposed method has the potential for analysis of mercury in water and soil samples without interference by possible foreign species.

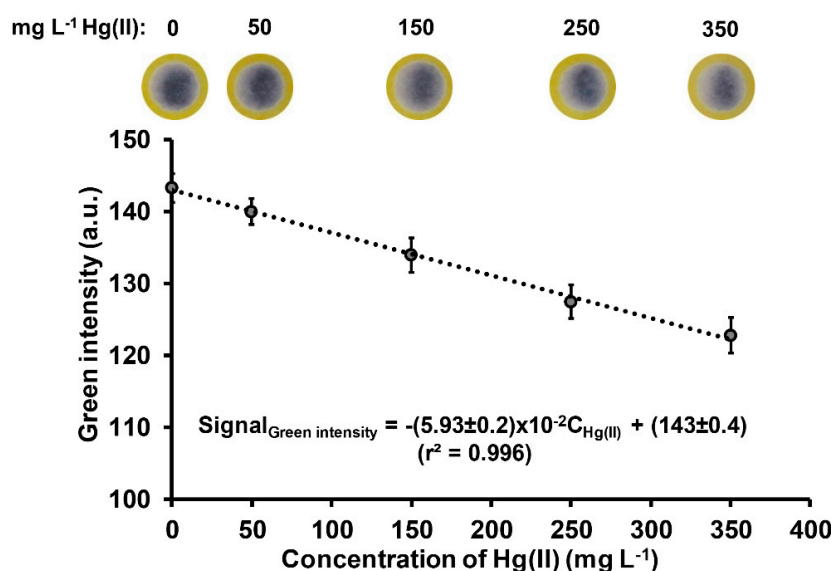


Figure 5. Calibration line using the membraneless gas-separation μ PAD for the determination of mercury and the corresponding image of the purple iodine-starch complex.

Table 2. The tolerance limit of the μ PAD for analysis of Hg(II) and comparison with the reported levels of foreign species in some samples (drinking water, river water and soil).

Foreign Species	Reported Level		Tolerance Limit (mg L^{-1})
	River Water (mg L^{-1}) ^a	Soil (mg kg^{-1}) ^b	
Copper (II)	0.006–10	5–70	1000 ^c
Lead (II)	0.003–0.3	10–67	1000 ^c
Cadmium (II)	0.01–0.04	6.4–11.7	1000 ^c
Iron (II)	0.03–0.05	0.5–10	1000 ^c
Nitrate (NO_3^-)	5–50	8–119	1000 ^c
Sulfate (SO_4^{2-})	–	29–130	1000 ^c
Cyanide (CN^-)	≤ 0.2	11–44	750
Chromium (III)	0.05–0.2	2–60	500
Zinc (II)	0.05–0.1	8.9–65.7	500
Nickel (II)	0.03–10	3–100	500
Iron (III)	≤ 7	20–30	250
Silver (I)	0.3–1	0.2–0.3	250
Sulfide (S^{2-})	Up to 0.05	Up to 11.7	25

^a Reported by World Health Organization, 2011. [40]; ^b Reported by Fashola et al. [41]; ^c Maximum tested concentration.

2.5. Applications and Validation

Three soil samples (S1–S3) were obtained from artisanal small-scale gold mining (ASGM) areas on Lombok Island, Indonesia. The other soil samples (S4–S10) were collected from Bangkok City and Samut Sakorn Province, Thailand. Water samples were collected from canals in Bangkok, Thailand. Soil samples were first digested using USEPA 3050B [42] standard method and the water samples were treated as described in Section 3.2.

Table 3 gives the amount of Hg(II) obtained from samples of the soil and water, as the concentration of the sample solution (mg L^{-1} Hg) loaded on the membraneless gas-separation μPAD (Step 2 in Figure 2). Examples of the images of the colored product that was formed in the acceptor reservoir during analysis of soil and water samples are depicted in Figure S3 (see the supplementary data). Only soil samples S1–S3 were found to have Hg(II) levels. Converting the values in Table 3 to mg kg^{-1} soil sample, the amounts are 3041, 3166 and 3151 mg kg^{-1} Hg, respectively. The mercury contents in all contaminated soils are above World Health Organization (WHO) limits for agricultural soils (0.05 mg kg^{-1}) [43].

Table 3. Percentage recovery of mercury in soil and water samples using the μPAD .

Sample	Mercury Concentration (mg L^{-1} Hg)			% Recovery
	Present ^a	Added	Found ^b	
Soil Sample				
S1	121.7 ± 5.3	50	174.4 ± 4.5	105.5
S2	126.7 ± 4.3	50	175.2 ± 3.4	97.0
S3	126.1 ± 3.7	50	180.2 ± 4.2	108.2
S4	n.d.	100	105.4 ± 3.6	105.4
S5	n.d.	100	96.9 ± 3.6	96.9
S6	n.d.	100	96.7 ± 4.9	96.7
S7	n.d.	100	104.1 ± 4.3	104.1
S8	n.d.	100	100.3 ± 3.8	100.3
S9	n.d.	100	103.5 ± 4.6	103.5
S10	n.d.	100	105.7 ± 3.7	105.7
Water Sample				
W1	n.d.	100	90.7 ± 3.9	90.7
W2	n.d.	100	101.2 ± 3.5	101.2
W3	n.d.	100	97.2 ± 2.9	97.2
W4	n.d.	100	102.9 ± 3.2	102.9

^a Mean concentration \pm SD, $n = 3$. ^b Concentration of sample after spiking with standard solution; n.d.: Not detected.

Percent recoveries of spiked mercury in soil and water samples were carried out using the developed μPAD . All samples were spiked at 100 mg L^{-1} Hg, except for soil samples S1 to S3 which were spiked at 50 mg L^{-1} Hg. As shown in Table 3, the recoveries were 96.7–108.2% and 90.7–102.9% for soil and water samples, respectively. According to the AOAC guideline [44], the recovery values are in the acceptable range.

The concentrations of mercury in the soil and water samples were also analyzed using inductively coupled plasma mass spectrometry (ICP-MS). The three digested soil samples (S1–S3) were analyzed directly using ICP-MS with appropriate dilution. The other digested soil samples (S4–S10) were spiked at 2500 mg kg^{-1} Hg, whereas water samples (W1–W4) were spiked at 100 mg L^{-1} Hg. Our method provides comparable results to the reference ICP-MS method (see Figure 6) as shown by using paired t -test at 95% confidence level ($t_{\text{stat}} = 1.38$, $t_{\text{crit}} = 2.16$). The results in Figure 6 suggest that our method is accurate and that the air-conditioning system provides good control of the temperature for gas diffusion inside μPADs .

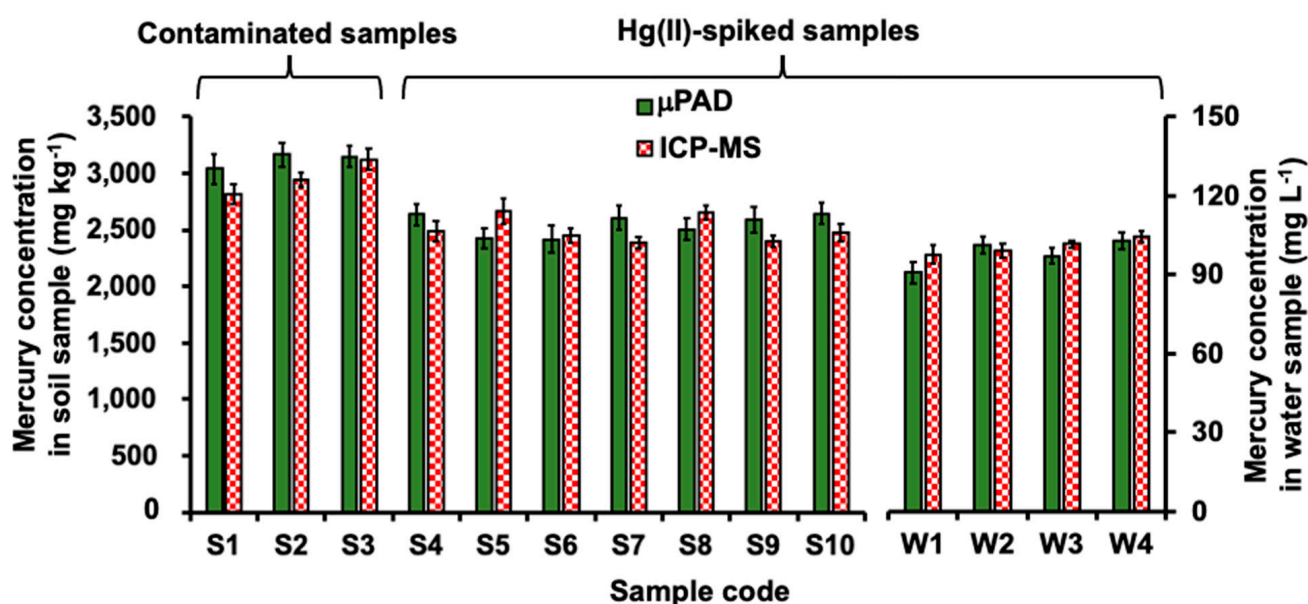


Figure 6. Bar plots of the concentrations of mercury in digested soil and water samples as determined using the membraneless gas-separation μ PAD and the reference ICP-MS method. The digested soil samples, S1–S3, were analyzed directly using ICP-MS with appropriate dilution. The other digested soil samples, S4–S10, were spiked at $2500 \text{ mg kg}^{-1} \text{ Hg}$. The water samples, W1–W4, were spiked at $100 \text{ mg L}^{-1} \text{ Hg}$.

2.6. Comparison of the Proposed Method with Existing Methods Including Other PADs/ μ PADs Methods for Determination of Mercury

Analytical features of the proposed method and previous methods are summarized in Table 4. Cold vapor-AAS technique (Technique No. 1 in Table 4) is usually the gold standard method that utilizes a very reliable equipment, the atomic absorption spectrophotometer. In this method, mercury in water or soil samples is reduced using SnCl_2 or NaBH_4 to form Hg^0 [7,9,45]. However, during the procedure, the generated Hg^0 vapor is prone to be released into the workplace which causes a health risk for the operator. Apart from the equipment-based techniques, like the cold vapor-AAS, there are alternative ways to analyze mercury without liberating Hg^0 and without use of equipment, viz. using paper-based analytical techniques. These paper-based techniques include both PADs and μ PADs which are listed in Table 4 as techniques No. 2.1–2.3 and techniques No. 3.1–3.4. The strategy of techniques No. 2.1–2.3 exploit the special features of nanoparticles (both unmodified [26,27,30] and functionalized synthesized [28,29]) to enhance the sensitivity of mercury detection. Nonetheless, the use of nanoparticles also has the problem of possible ecological issue since it is easily released into the environment [46]. Risks of nanoparticles to human health have always been an issue of public concern along with the advantages in their applications [47]. Techniques No. 3.1 to 3.3 in Table 4 show PADs/ μ PADs techniques that were developed without using nanoparticles. Instead, these techniques utilized a chemical reaction to form a colored compound for semi-quantitative [24] or quantitative analyses of mercury [25,31]. Although these techniques do not produce Hg^0 , the chemicals employed are not eco-friendly.

Table 4. Comparison of the analytical features of various techniques for the determination of mercury.

Technique Class/Reagent	Test Samples	Working Range/LOD	Analysis Time (Excluding Sample Preparation)	Classified as "Equipment-Free" Method	Remark
1. Cold vapor-AAS/ SnCl ₂ , NaBH ₄ , KMnO ₄ (for hydride generation)	• Water [45]	0.04–2.4 µg L ⁻¹ Hg/0.02 µg L ⁻¹ Hg	NR ^a	} No	All reagents are commercially available. Hg vapor is generated.
	• Soil [9]	5–40 µg L ⁻¹ Hg/0.01 µg L ⁻¹ Hg	NR ^a		
	• Soil and sediment [7]	1–30 µg L ⁻¹ Hg/0.08 mg kg ⁻¹	NR ^a		
2. Colorimetric µPADs or PADs with NPs/					
2.1 Functionalized AuNPs, TMB, H ₂ O ₂	• Tap water (spiked) [29]	0.2–2000 ng Hg/30 µg L ⁻¹ Hg	10 min	} Yes	The factionalized AuNPs are not yet commercialized.
2.2 Synthesized-AgNPs	• Drinking water (spiked), tap water (spiked) [30]	0.01–10 mg L ⁻¹ Hg/0.003 mg L ⁻¹ Hg	12 min		
	• Drinking water (spiked), tap water (spiked) [26]	0.05–7 mg L ⁻¹ Hg/0.001 mg L ⁻¹ Hg	NR		
	• Drinking water (spiked), tap water (spiked) [27]	5–75 mg L ⁻¹ Hg/0.12 mg L ⁻¹ Hg	45 min		
2.3 Synthesized-CcNPs	• Industrial water (spiked) [28]	0.5–20 mg L ⁻¹ Hg/0.17 mg L ⁻¹ Hg	15 min	} Yes	CcNPs are not yet commercialized.
3. Colorimetric µPADs or PADs without NPs/					
3.1 Dithizone in CCl ₄	• Synthetic water, whitening cream extract [31]	1–30 mg L ⁻¹ Hg/0.93 mg L ⁻¹ Hg	≥10 min	} Yes	Not eco-friendly reagent/solvent.
3.2 Resorufin thiono-carbonate in CH ₂ Cl ₂	• Simulated wastewater [25]	2–10 mg L ⁻¹ Hg/1.18 mg L ⁻¹ Hg	NR		Not eco-friendly reagent/solvent.
3.3 Rhodamine derivatives in CH ₂ Cl ₂	• NONE [24]	20, 50, 100, 200, 300 mg L ⁻¹ Hg (no calibration plot)/NR	≥15 min		Need synthesized chemicals. Not eco-friendly solvent.
3.4 <i>This work/</i> KI, KIO ₃ , H ₂ SO ₄ , starch	• Water (spiked) • Soil (from gold mining)	50–300 mg L ⁻¹ Hg/20 mg L ⁻¹ Hg	10 min		All reagents are common and are all commercially available. No serious toxicity from skin exposure (KI, KIO ₃ , starch) except 0.2 mol L ⁻¹ H ₂ SO ₄ .

NR: Not reported; TMB: 3,3',5,5'-tetramethylbenzidine; CcNPS: Curcumin nanoparticles. ^a Usual analysis time for cold vapor-AAS is 3 min with use of flow injection system [48].

It is also observed from Table 4 that all PADs/ μ PADs techniques developed in the last decade [25–31] were tested only in water samples (all spiked with mercury), which are not as complicated as soil. There were no alternative methods to the cold vapor-AAS for assessing soil contamination particularly for use in countries with limited resources. Our mercury μ PAD was developed with the purpose of analysis of soil samples. Although our method provides less sensitivity compared to others μ PADs method, the detection limit is sufficient for determination of mercury in soils from contaminated areas. The results in Figure 6 show that our μ PAD is capable of analyzing real soil samples collected from artisanal small-scale gold mining areas. We also successfully validated our μ PAD method for water analysis. As shown in the remark column of Table 4, our technique (techniques No. 3.4) employs very common reagents which are not hazardous. The chemicals can be easily obtained from worldwide suppliers at economic prices. The analysis time of our μ PAD is comparable with most PADs/ μ PADs techniques [28–30] (10–15 min/analysis). Comparing to PAD technique No. 2.2, which is the pioneering work in utilizing AgNPs in paper-based devices for mercury [27], our method gives a much faster analysis time (10 min compared to 45 min).

3. Materials and Methods

3.1. Chemicals and Reagents

Chemicals used in this work were all analytical reagent (AR) grade. Deionized water (18.2 M Ω -cm, Thermo Scientific Easypure II system, Waltham, MA, USA), was employed for the preparation of all aqueous solutions. All of the glassware and the bottles were cleaned, rinsed with deionized water, soaked overnight in 10% (*v/v*) nitric acid, then rinsed with deionized water.

A standard stock solution of Hg(II) (10.0 g L⁻¹ Hg) was prepared by dissolving an accurate weight of 1.36 g of mercuric chloride powder (Ajax Finechem., Australia) in 0.01 mol L⁻¹ of nitric acid (RCI Lab Scan, Thailand) in a 100 mL volumetric flask. Working standard solutions of mercury were prepared by subsequent dilution of this stock solution with 0.01 mol L⁻¹ nitric acid. A stock solution of 0.5 mol L⁻¹ potassium iodate was prepared by dissolving 1.07 g of potassium iodate powder (Ajax Finechem.) in 100 mL of deionized water. This solution was used for preparing the oxidizing agent for iodometric reaction (at donor reservoir 'dr'), which is a mixture of 0.2 mol L⁻¹ potassium iodate and 0.2 mol L⁻¹ sulphuric acid. The solution was freshly prepared daily by mixing 4 mL of 0.5 mol L⁻¹ potassium iodate and 4 mL of 0.5 mol L⁻¹ sulphuric acid (RCI Lab Scan, Thailand) and then made up to 10 mL with deionized water. Potassium iodide solution is used for forming the HgI₄²⁻ complex at the sample reservoir ('sr' in Figure 2). A stock solution of 0.1 mol L⁻¹ potassium iodide was firstly prepared by dissolving 1.66 g of potassium iodide crystal (Merck, Germany) in 100.0 mL of deionized water. The solution of 10 mmol L⁻¹ potassium iodide was prepared by diluting this stock solution 10-fold with deionized water. The solution of 1% (*w/v*) of starch in 0.1 mol L⁻¹ potassium iodide was used as the color forming reagent at the acceptor reservoir ('ar' in Figure 2). The solution was freshly prepared daily by dissolving 0.05 g of starch powder (BDH, U.K.) in 5 mL boiling deionized water and then letting the solution cool to room temperature before adding 0.083 g potassium iodide crystal.

3.2. Preparation of Samples

The water samples were filtered with Whatman filter paper No. 42 (Whatman International, Ltd., Maidstone, UK) followed by acidification with nitric acid to pH 2. For soil samples, the wet soil/sediments were placed in a petri dish and air dried for 48 h. The dried soil samples were ground with a mortar and pestle and then heated in an oven at 120° C for 2 h. After cooling to room temperature, the samples were stored in a desiccator until analyzed. The soil samples were acid digested prior to analysis. The USEPA 3050B protocol of the standard acid method for determination of heavy metals in soil samples [42] was adopted for this work. Previous comparison study [49] have shown that there is an

acceptable correlation ($r = 0.99$) between the USEPA 3050B protocol (open system digestion) and the USEPA 3051A protocol (close system digestion by microwave) for determination of mercury in 10 classes of soils. Briefly, 2 g of soil was placed in a Teflon beaker; then, 5 mL of concentrated HNO_3 was added and the beaker covered with a watch glass. The solution was then heated on a hotplate at 95 ± 5 °C for 15 min and cooled to room temperature. Another 5 mL of concentrated HNO_3 was added and heated again at 95 ± 5 °C for 2 h. After cooling 2 mL of deionized water and 3 mL of 30% hydrogen peroxide (Sigma-Aldrich, Germany) were added, followed by the heating step for a further 2 h. The last step of digestion was the addition of 10 mL of hydrochloric acid (RCI Lab Scan, Thailand) with heating for 15 minutes at 95 ± 5 °C. The digested solution was filtered with 0.45 μm of cellulose acetate membrane and adjusted to pH 2 using a few drops of 50% (w/v) sodium hydroxide. The filtered solution was made up in a 50 mL volumetric flask with deionized water. This solution was used for the determination of mercury using the membraneless gas-separation μPAD . Appropriate dilution of the filtrate with 2% (v/v) sub-boiled nitric acid was performed prior to determination of Hg in the samples by inductively coupled plasma mass spectrometry (ICP-MS 7900, Agilent Technologies, Santa Clara, CA, USA) as the comparison method.

3.3. Fabrication of μPAD

The membraneless gas-separation μPAD comprises 3 layers: a donor layer, a spacer layer and an acceptor layer. Two patterns of the hydrophobic barriers were employed, as shown in Figure 1a: a single circular pattern for the donor layer and a dumbbell-shaped pattern with 2 different sizes of the reservoirs for the donor layer. The sample reservoir ('sr') and the acceptor reservoir ('ar') were of the same dimension of 6 mm i.d., whereas the second donor reservoir ('dr') has 3 mm i.d. The spacer layer was a mounting tape with 0.8 mm thickness (Scotch™, St. Paul, MN, USA) which has a 7 mm circular disc cut out. The donor layer, spacer layer and acceptor layer were assembled together to produce the membraneless gas-separation μPAD as shown in Figure 1b. Figure 1c shows the assembled μPAD from the acceptor and donor side, respectively. The printed circular hydrophobic barriers are screen-printed on a Whatman No. 4 filter paper (Maidstone, UK), following the method of Sitanurak et al. [33], to define the circular reservoirs for the donor and acceptor layers, respectively. The patterned paper was kept overnight at the room temperature for complete curing of the resin prior to cutting to give separate devices. One screen-printed paper provides 77 pads. These μPAD devices are stable for at least 2 years.

3.4. Operating Procedure

The operating procedure for using the membraneless gas-separation μPAD to measure the amount of Hg(II) is shown in Figure 2. The analysis is carried out at room temperature in an air-conditioned room (26–27 °C). In the first step (Step 1), 1.0 μL of the oxidizing agent (0.2 mol L^{-1} KIO_3 in 0.2 mol L^{-1} H_2SO_4) is loaded on the donor reservoir 'dr' using an autopipette (Rainin Instrument, Mettler Toledo, Switzerland), followed by (Step 2), the addition of 3.0 μL Hg(II) standard/sample on to the sample reservoir 'sr' and then waiting ca. 5 min for the pad to dry. Next, the device is turned over and (Step 3) 2.0 μL of the color developing reagent (1% (w/v) starch in 0.1 mol L^{-1} KI) is loaded on the acceptor reservoir 'ar'. The acceptor reservoir 'ar' and donor reservoir 'dr' are then immediately covered with transparent adhesive tape (Scotch™) (Step 4) to prevent loss of the reagents from the device. Next, (Step 5), 8.0 μL of 10 mmol L^{-1} KI is loaded on the sample reservoir 'sr'. The iodide solution reacts with Hg(II) deposited earlier (in Step 2) forming the colorless HgI_4^{2-} complex at the 'sr' reservoir. The unreacted iodide diffuses into reservoir 'dr', where it is converted to volatile iodine ($\text{I}_{2(g)}$) by iodate ion deposited earlier (in Step 1). The iodine gas diffuses across the spacer to react with the starch-KI reagent on the acceptor side (Step 3) to generate the purple color of triiodide-starch complex. In the final step (Step 6) the acceptor layer is placed face up inside an in-house light-box (fitted with a JMF fs-wh-1 watt LED light tube). The image of the purple color complex is recorded at 4 min after the addition

of KI (Step 5 in Figure 2) using a digital camera (IXUS 125 HS, Canon, Japan). The color intensity of the image is analyzed using ImageJ software (version v1.35e). The green color scale is used to construct the calibration line for concentrations of Hg(II) in the standard solutions. Note: The volume of sample of 3.0 μL was chosen to provide the maximum loading of the sample into the sample reservoir 'sr' without the overflow of sample into the donor reservoir 'dr'.

4. Conclusions

A simple, cost-effective, equipment-free and environmentally friendly μPAD method was developed for determination of Hg(II) in contaminated soil and water samples by using a membraneless gas-separation μPAD . Mercury in the sample is determined by an indirect colorimetric procedure. The detection principle is based on quantitating the color image of I_3^- -starch complex. In the donor layer of the membraneless gas-separation μPAD , the pre-deposited sample containing mercuric ions reacts with an added solution containing a fixed amount of excess iodide to form the colorless complex of HgI_4^{2-} . The remaining iodide flows to a connected adjacent area, where it is oxidized by acidic iodate to produce volatile iodine via the Dushman reaction [50]. The volatile iodine moves across an air spacer region to react with pre-deposited iodide-starch to form the purple I_3^- -starch complex at the acceptor layer. This method is applicable for measurement of high concentrations of mercury, especially in contaminated soil and water in artisanal small-scale gold mining area.

The method fits the purpose for waste management of contaminated sites in many developing countries where artisanal small-scale gold mining is still an important primary economic sector (e.g., Asia, Africa and South America) [2]. Our developed μPAD for mercury detection has several advantages. The fabrication of μPAD by screen-printing technique is simple and does not require sophisticated skill. Hence, this mercury μPAD can be produced anywhere in the world where filter paper, double-sided mounting tape, screen-printing tools, t-shirt ink (as hydrophobic barrier) are available. The production cost is approximately 7 US\$/100 devices [33] which is suitable for developing countries. Moreover, our method is in compliance with "Green Analytical Chemistry", since there is reduction of waste generation (e.g., no hazardous synthesis), with low human toxicity and eco-toxicity.

Supplementary Materials: The following is available online. Method S1: Preliminary test for selection of the color scale; Figure S1: Calibration graphs obtained from preliminary tests using the iodine-starch reaction on a single-layer paper device with the ImageJ analysis of the plot between (a) grey intensity, (b) red intensity, (c) green intensity and (d) blue intensity against the concentration of iodide.; Method S2: Control of light illumination and calibration of camera; Figure S2: Effect of pH of standard 150 mg L^{-1} Hg solutions on the green intensity value. Experimental conditions: 0.2 mol L^{-1} KIO_3 in 0.2 mol L^{-1} H_2SO_4 , 10 mmol L^{-1} KI, 1% (w/v) of starch in 0.1 mmol L^{-1} KI and reaction time of 4 min.; Figure S3: Examples of photographic images of the colored product formed in the acceptor reservoirs during analysis of soil and water samples. Note: Soil samples S1–S3 were highly contaminated with mercury whereas the levels of mercury in other samples of soils and waters are below the detection limit.

Author Contributions: Conceptualization, K.U. and D.N.; methodology, K.U., H.L.N. and J.S.; validation, K.U. and H.L.N.; investigation, K.U.; resources, K.U.; writing original draft preparation, H.L.N.; writing review and editing, K.U. and D.N.; visualization, K.U.; supervision, D.N. and H.S.; project administration, K.U.; funding acquisition, K.U. and D.N. All authors have read and agreed to the published version of the manuscript.

Funding: This research was supported by the National Research Council of Thailand (IRN/502/2563) chaired by Assoc. Prof. Dr. Duangjai Nacapricha and the Center of Excellence for Innovation in Chemistry (PERCH-CIC), Ministry of Higher Education, Science, Research and Innovation and the International Foundation for Science (IFS).

Institutional Review Board Statement: Not applicable.

Informed Consent Statement: Not applicable.

Data Availability Statement: The data presented in this study, are available on request from the corresponding authors.

Acknowledgments: The authors would like to thank the support of equipment from the CIF Grant, Faculty of Science, Mahidol University. Finally, the authors would like to thank Prapin Wilairat for his useful comments and editing.

Conflicts of Interest: The authors declare no conflict of interest.

Sample Availability: Samples of the compounds are available from the authors.

References

1. United States Environmental Protection Agency. *EPA-452/R-97-004, Mercury Study Report to Congress, Volume II: An Inventory of Anthropogenic Mercury Emissions in the United States*; U.S. Environmental Protection Agency: Washington, DC, USA, 1997.
2. United Nations Environment Programme. *A Practical Guide: Reducing Mercury Use in Artisanal and Small-Scale Gold Mining*; UNEP: Geneva, Switzerland, 2013.
3. Esdaile, L.J.; Chalker, J.M. The mercury problem in artisanal and small-scale gold mining. *Chem. Eur. J.* **2018**, *24*, 6905–6916. [[CrossRef](#)] [[PubMed](#)]
4. Park, J.D.; Zheng, W. Human exposure and health effects of inorganic and elemental mercury. *J. Prev. Med. Public Health* **2012**, *45*, 344–352. [[CrossRef](#)] [[PubMed](#)]
5. United States Environmental Protection Agency. *Method 245.1, Revision 3.0: Determination of Mercury in Water by Cold Vapor Atomic Absorption Spectrometry*; U.S. Environmental Protection Agency: Washington, DC, USA, 1994.
6. United States Environmental Protection Agency. *Method 7471B, Mercury in Solid or Semisolid Waste (Manual Cold-Vapor Technique)*; U.S. Environmental Protection Agency: Washington, DC, USA, 1998.
7. Almeida, I.L.S.; Oliveira, M.D.R.; Silva, J.B.B.; Coelho, N.M.M. Suitable extraction of soils and sediments for mercury species and determination combined with the cold vapor generation atomic absorption spectrometry technique. *Microchem. J.* **2016**, *124*, 326–330. [[CrossRef](#)]
8. Kodamatani, H.; Tomiyasu, T. Selective determination method for measurement of methylmercury and ethylmercury in soil/sediment samples using high-performance liquid chromatography–chemiluminescence detection coupled with simple extraction technique. *J. Chromatogr. A* **2013**, *1288*, 155–159. [[CrossRef](#)]
9. Krata, A.; Bulska, E. Critical evaluation of analytical performance of atomic absorption spectrometry and inductively coupled plasma mass spectrometry for mercury determination. *Spectrochim. Acta B* **2005**, *60*, 345–350. [[CrossRef](#)]
10. Jiang, Z.; Wen, G.; Fan, Y.; Jiang, C.; Liu, Q.; Huang, Z.; Liang, A. A highly selective nanogold-aptamer catalytic resonance scattering spectral assay for trace Hg²⁺ using HAuCl₄-ascorbic acid as indicator reaction. *Talanta* **2010**, *80*, 1287–1291. [[CrossRef](#)]
11. Ackermann, G.; Roder, H. Photometrische Bestimmung von Quecksilber(II) im Nanogrammbereich mit Thio-Michlers Keton. *Talanta* **1977**, *24*, 99–103. [[CrossRef](#)]
12. Tupys, A.; Kalemkiewicz, J.; Bazel, Y.; Zapala, L.; Dranka, M.; Ostapiuk, Y.; Tymoshuk, O.; Woźnicka, E. 1-[(5-Benzyl-1,3-thiazol-2-yl)diazetyl]naphthalene-2-ol: X-ray structure, spectroscopic characterization, dissociation studies and application in mercury(II) detection. *J. Mol. Struct.* **2017**, *1127*, 722–733. [[CrossRef](#)]
13. Prasertboonyai, K.; Liawraungrath, B.; Pojanakaroon, T.; Liawraungrath, S. Mercury(II) determination in commercial cosmetics and local Thai traditional medicines by flow injection spectrophotometry. *Int. J. Cosmet. Sci.* **2016**, *38*, 68–76. [[CrossRef](#)]
14. Tarighat, M.A.; Mohammadi, K. Simultaneous spectrophotometric determination of Cu²⁺, Hg²⁺, and Cd²⁺ ions using 2-(3-hydroxy-1-methylbut-2-enylideneamino) pyridine-3-ol. *Environ. Monit. Assess.* **2015**, *187*, 197. [[CrossRef](#)]
15. Meng, S.; Wang, J.; Fan, Y.; Zhao, Q.; Guo, Y. Spectrophotometric determination of trace mercury(II) in cereals with 2,4-bis(4-phenylazophenylaminodiazo) benzenesulfonic acid. *J. Anal. Chem.* **2013**, *68*, 488–494. [[CrossRef](#)]
16. Huang, D.; Liu, X.; Lai, C.; Qin, L.; Zhang, C.; Yi, H.; Zeng, G.; Li, B.; Deng, R.; Liu, S.; et al. Colorimetric determination of mercury(II) using gold nanoparticles and double ligand exchange. *Microchim. Acta* **2019**, *186*, 31. [[CrossRef](#)] [[PubMed](#)]
17. Kataria, R.; Sethuraman, K.; Vashisht, D.; Vashisht, A.; Mehta, S.K.; Gupta, A. Colorimetric detection of mercury ions based on anti-aggregation of gold nanoparticles using 3, 5-dimethyl-1-thiocarboxamidepyrazole. *Microchem. J.* **2019**, *148*, 299–305. [[CrossRef](#)]
18. Kong, Y.; Shen, J.; Fan, A. Colorimetric method for the detection of mercury ions based on gold nanoparticles and mercaptophenyl boronic acid. *Anal. Sci.* **2017**, *33*, 925–930. [[CrossRef](#)]
19. Kaneta, T.; Alahmad, W.; Varanusupakul, P. Microfluidic paper-based analytical devices with instrument-free detection and miniaturized portable detectors. *Appl. Spectrosc. Rev.* **2019**, *54*, 117–141. [[CrossRef](#)]
20. Almeida, M.I.G.S.; Jayawardane, B.M.; Kolev, S.D.; McKelvie, I.D. Developments of microfluidic paper-based analytical devices (μPADs) for water analysis: A review. *Talanta* **2018**, *177*, 176–190. [[CrossRef](#)]
21. Yang, Y.; Noviana, E.; Nguyen, M.P.; Geiss, B.J.; Dandy, D.S.; Henry, C.S. Paper-based microfluidic devices: Emerging themes and applications. *Anal. Chem.* **2017**, *89*, 71–91. [[CrossRef](#)]

22. Ozer, T.; McMahon, C.; Henry, C.S. Advances in paper-based analytical devices. *Annu. Rev. Anal. Chem.* **2020**, *13*, 85–109. [[CrossRef](#)] [[PubMed](#)]
23. Boobphahom, S.; Ly, M.N.; Soum, V.; Pyun, N.; Kwon, O.; Rodthongkum, N.; Shin, K. Recent advances in microfluidic paper-based analytical devices toward high-throughput screening. *Molecules* **2020**, *25*, 2970. [[CrossRef](#)] [[PubMed](#)]
24. Patidar, R.; Rebarry, B.; Paul, P. Colorimetric and fluorogenic recognition of Hg²⁺ and Cr³⁺ in acetonitrile and their test paper recognition in aqueous media with the aid of rhodamine based sensors. *J. Fluoresc.* **2015**, *25*, 387–395. [[CrossRef](#)]
25. Choi, M.G.; Park, S.Y.; Park, K.Y.; Chang, S.K. Novel Hg²⁺-selective signaling probe based on resorufin thionocarbonate and its μ PAD application. *Sci. Rep.* **2019**, *9*, 3348. [[CrossRef](#)] [[PubMed](#)]
26. Meelapsom, R.; Jarujamrus, P.; Amatongchai, M.; Chairam, S.; Kulsing, C.; Shen, W. Chromatic analysis by monitoring unmodified silver nanoparticles reduction on double layer microfluidic paper-based analytical devices for selective and sensitive determination of mercury(II). *Talanta* **2016**, *155*, 193–201. [[CrossRef](#)] [[PubMed](#)]
27. Apilux, A.; Siangproh, W.; Praphairaksit, N.; Chailapakul, O. Simple and rapid colorimetric detection of Hg(II) by a paper-based device using silver nanoplates. *Talanta* **2012**, *97*, 388–394. [[CrossRef](#)]
28. Pourreza, N.; Golmohammadi, H.; Rastegarzadeh, S. Highly selective and portable chemosensor for mercury determination in water samples using curcumin nanoparticles in a paper based analytical device. *RSC Adv.* **2016**, *6*, 69060–69066. [[CrossRef](#)]
29. Han, K.N.; Choi, J.S.; Kwon, J. Gold nanozyme-based paper chip for colorimetric detection of mercury ions. *Sci. Rep.* **2017**, *7*, 2806. [[CrossRef](#)]
30. Jarujamrus, P.; Meelapsom, R.; Pencharee, S.; Obma, A.; Amatongchai, M.; Ditcharoen, N.; Chairam, S.; Tamuang, S. Use of a smartphone as a colorimetric analyzer in paper-based devices for sensitive and selective determination of mercury in water samples. *Anal. Sci.* **2018**, *34*, 75–81. [[CrossRef](#)] [[PubMed](#)]
31. Cai, L.; Fang, Y.; Mo, Y.; Huang, Y.; Xu, C.; Zhang, Z.; Wang, M. Visual quantification of Hg on a microfluidic paper-based analytical device using distance-based detection technique. *AIP Adv.* **2017**, *7*, 085214. [[CrossRef](#)]
32. Phansi, P.; Sumantakul, S.; Wongpakdee, T.; Fukana, N.; Ratanawimarnwong, N.; Sitanurak, J.; Nacapricha, D. Membraneless gas-separation microfluidic paper-based analytical devices for direct quantitation of volatile and nonvolatile compounds. *Anal. Chem.* **2016**, *88*, 8749–8756. [[CrossRef](#)] [[PubMed](#)]
33. Sitanurak, J.; Fukana, N.; Wongpakdee, T.; Thepchuay, Y.; Ratanawimarnwong, N.; Amornsakchai, T.; Nacapricha, D. T-shirt ink for one-step screen-printing of hydrophobic barriers for 2D- and 3D-microfluidic paper-based analytical devices. *Talanta* **2019**, *205*, 120113. [[CrossRef](#)]
34. Skoog, D.A.; West, D.M.; Holler, F.J. *Fundamentals of Analytical Chemistry*, 7th ed.; Saunders College Publishing: New York, NY, USA, 1997.
35. Sitanurak, J.; Wangdi, N.; Sonsa-ard, T.; Teerasong, S.; Amornsakchai, T.; Nacapricha, D. Simple and green method for direct quantification of hypochlorite in household bleach with membraneless gas-separation microfluidic paper based analytical device. *Talanta* **2018**, *187*, 91–98. [[CrossRef](#)]
36. Miretzky, P.; Bisinoti, M.C.; Jardim, W.F.; Rocha, J.C. Factors affecting Hg (II) adsorption in soils from the Rio Negro basin (Amazon). *Quim. Nova* **2005**, *28*, 438–443. [[CrossRef](#)]
37. Kim, C.S.; Rytuba, J.J.; Brown, G.E. EXAFS study of mercury(II) sorption to Fe- and Al-(hydr) oxides: I. Effects of pH. *J. Colloid Interface Sci.* **2004**, *271*, 1–15. [[CrossRef](#)]
38. Magnusson, B.; Örnemark, U. (Eds.) *Eurachem Guide: The Fitness for Purpose of Analytical Methods—A Laboratory Guide to Method Validation and Related Topics*, Section 6.2.4, 2nd ed; Available online: <http://www.eurachem.org> (accessed on 8 March 2021).
39. Malehase, T.; Daso, A.P.; Okonkwo, J.O. Determination of mercury and its fractionation products in samples from legacy use of mercury amalgam in gold processing in Randfontein, South Africa. *Emerg. Contam.* **2016**, *2*, 157–165. [[CrossRef](#)]
40. World Health Organization. *Guidelines for Drinking-Water Quality*, 4th ed.; IWA Publishing: London, UK, 2011.
41. Fashola, M.O.; Ngole-Jeme, V.M.; Babalola, O.O. Heavy metal pollution from gold mines: Environmental effects and bacterial strategies for resistance. *Int. J. Environ. Res. Public Health* **2016**, *13*, 1047. [[CrossRef](#)] [[PubMed](#)]
42. United State Environmental Protection Agency. *USEPA 3050B, Method 3050B. Acid Digestion of Sediments, Sludges and Soils*; U.S. Environmental Protection Agency: Washington, DC, USA, 1996.
43. World Bank. *Project Guidelines: Industry sector guidelines. Pollution Prevention and abatement Handbook*; The International Bank for Reconstruction and Development/The World Bank: Washinton, DC, USA, 1998.
44. AOAC Official Methods of Analysis. *Appendix F: Guidelines for Standard Method Performance Requirements*; AOAC International: Rockville, MD, USA, 2016; p. 9.
45. Pourreza, N.; Ghanemi, K. Determination of mercury in water and fish samples by cold vapor atomic absorption spectrometry after solid phase extraction on agar modified with 2-mercaptobenzimidazole. *J. Hazard. Mater.* **2009**, *161*, 982–987. [[CrossRef](#)]
46. Elsaesser, A.; Howard, C.V. Toxicology of nanoparticles. *Adv. Drug Deliv. Rev.* **2012**, *64*, 129–137. [[CrossRef](#)] [[PubMed](#)]
47. Crisponi, G.; Nurchi, V.M.; Lachowicz, J.I.; Peana, M.; Medici, S.; Zoroddu, M.A. *Toxicity of Nanoparticles: Etiology and Mechanisms (Book Chapter 18), Antimicrobial Nanoarchitectonics*; Elsevier: Amsterdam, The Neterlands, 2017; pp. 511–546.
48. Agemian, H.; Chau, A.S.Y. A method for the determination of mercury in sediments by the automated cold vapor atomic absorption technique after digestion. *Anal. Chim. Acta* **1975**, *75*, 297–303. [[CrossRef](#)]

-
49. Bezerra da Silva, Y.J.A.; Araújo do Nascimento, C.W.; Biondi, C.M. Comparison of USEPA digestion methods to heavy metals in soil samples. *Environ. Monit. Assess.* **2014**, *186*, 47–53. [[CrossRef](#)]
 50. Dushman, S. The rate of the reaction between iodic and hydriodic acids. *J. Phys. Chem.* **1904**, *8*, 453–482. [[CrossRef](#)]